Fachhochschule Nordwestschweiz

X-ray and EUV observations as diagnostic of accelerated electrons and atmospheric response in solar flares "

Marina Battaglia
Fachhochschule Nordwestschweiz (FHNW)
marina.battaglia@fhnw.ch

E. P. Kontar, G. Motorina, L. Kleint, S. Krucker, D. Graham

Overview

1. Solar flares: open questions

2. The standard solar flare scenario

3. Emission mechanisms at X-ray and EUV wavelengths

4. Electron acceleration: Distribution and energies of accelerated electrons from simultaneous EUV and X-ray analysis

5. Chromospheric response: chromospheric evaporation seen in X-rays and EUV

1. Summary and Conclusions

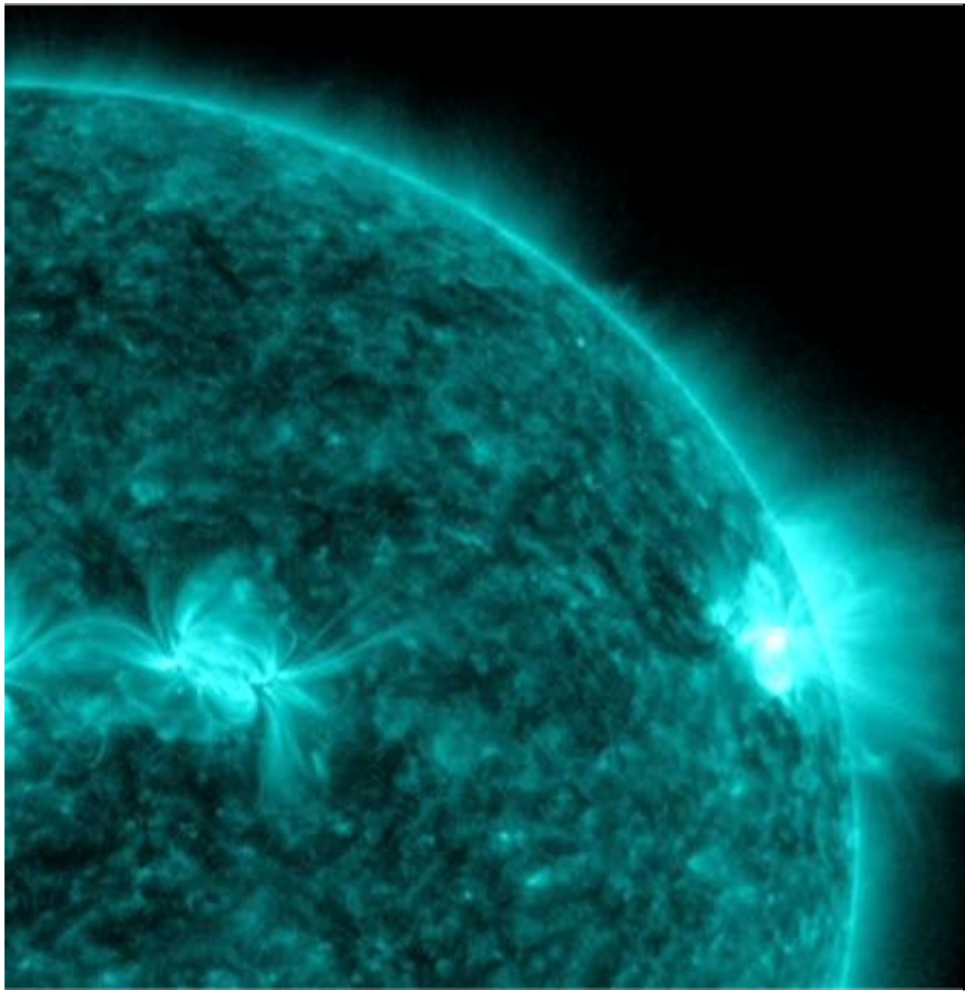

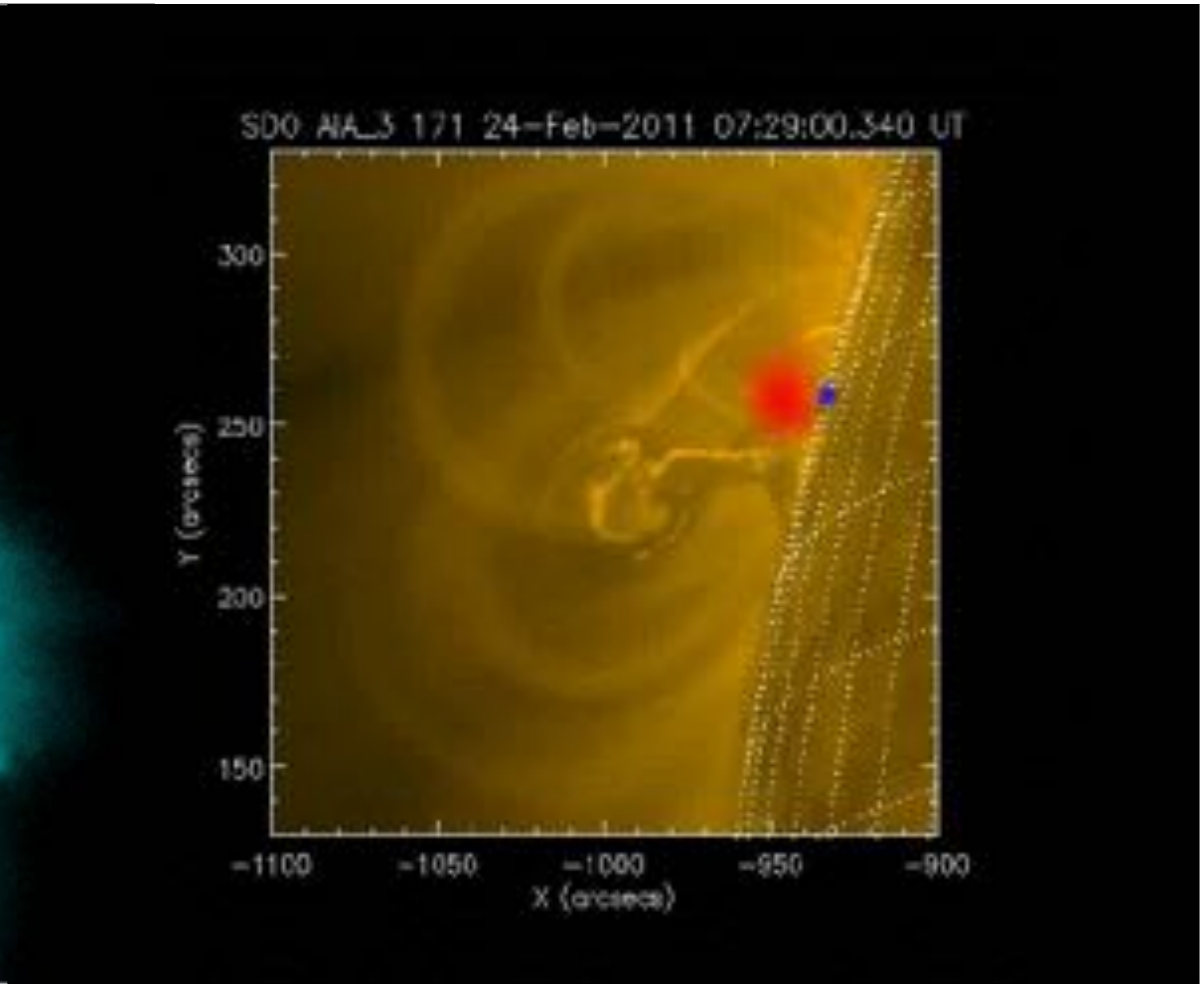
SDO AIA_3 171 24-Feb-2011 07:29:00.340 UT
Y (arcsecs)
300
250
200
150
-1100
-1050
-1000
-950
-900
X (arcsecs)

1. Solar flares: open questions

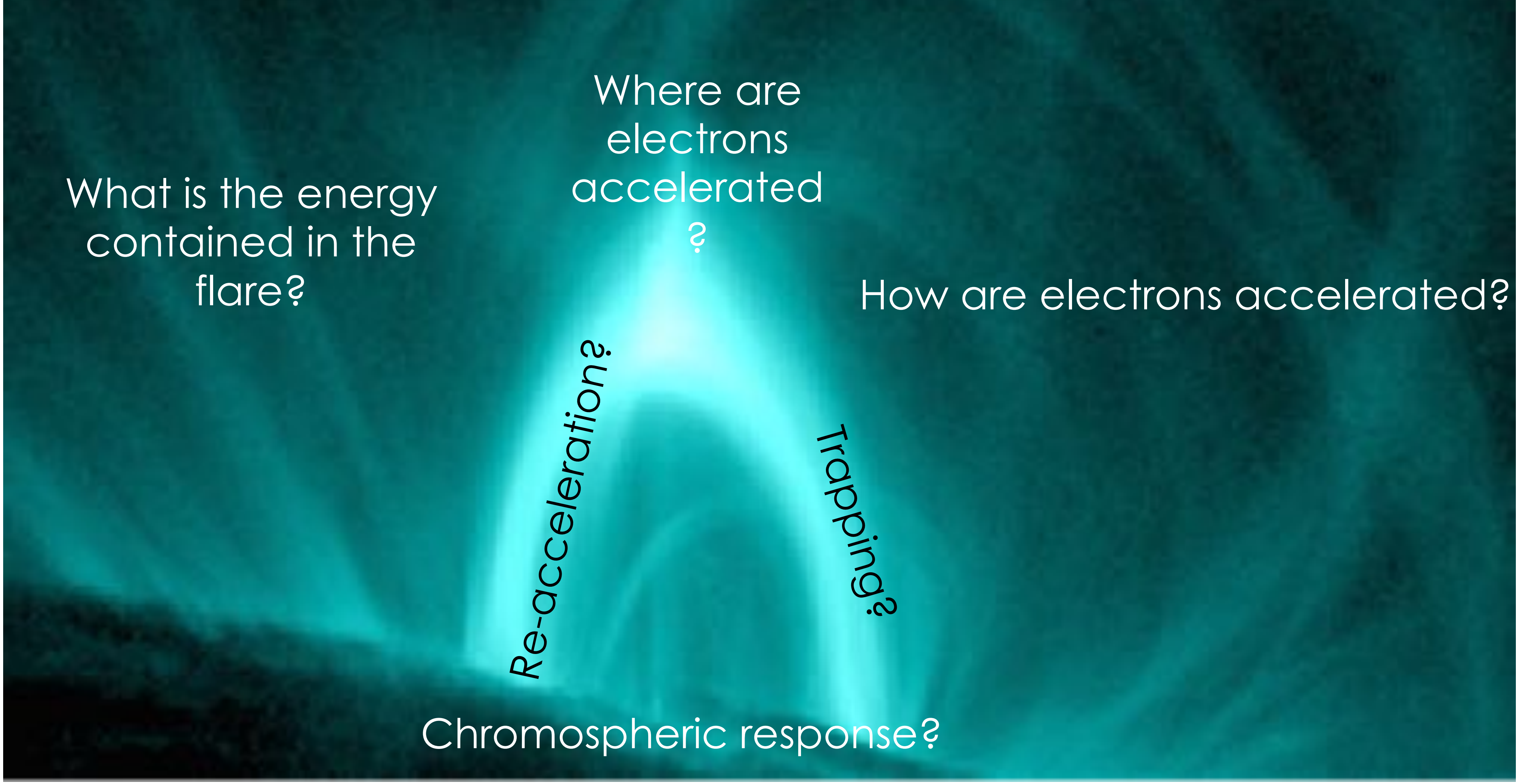

1. Solar flares: open questions

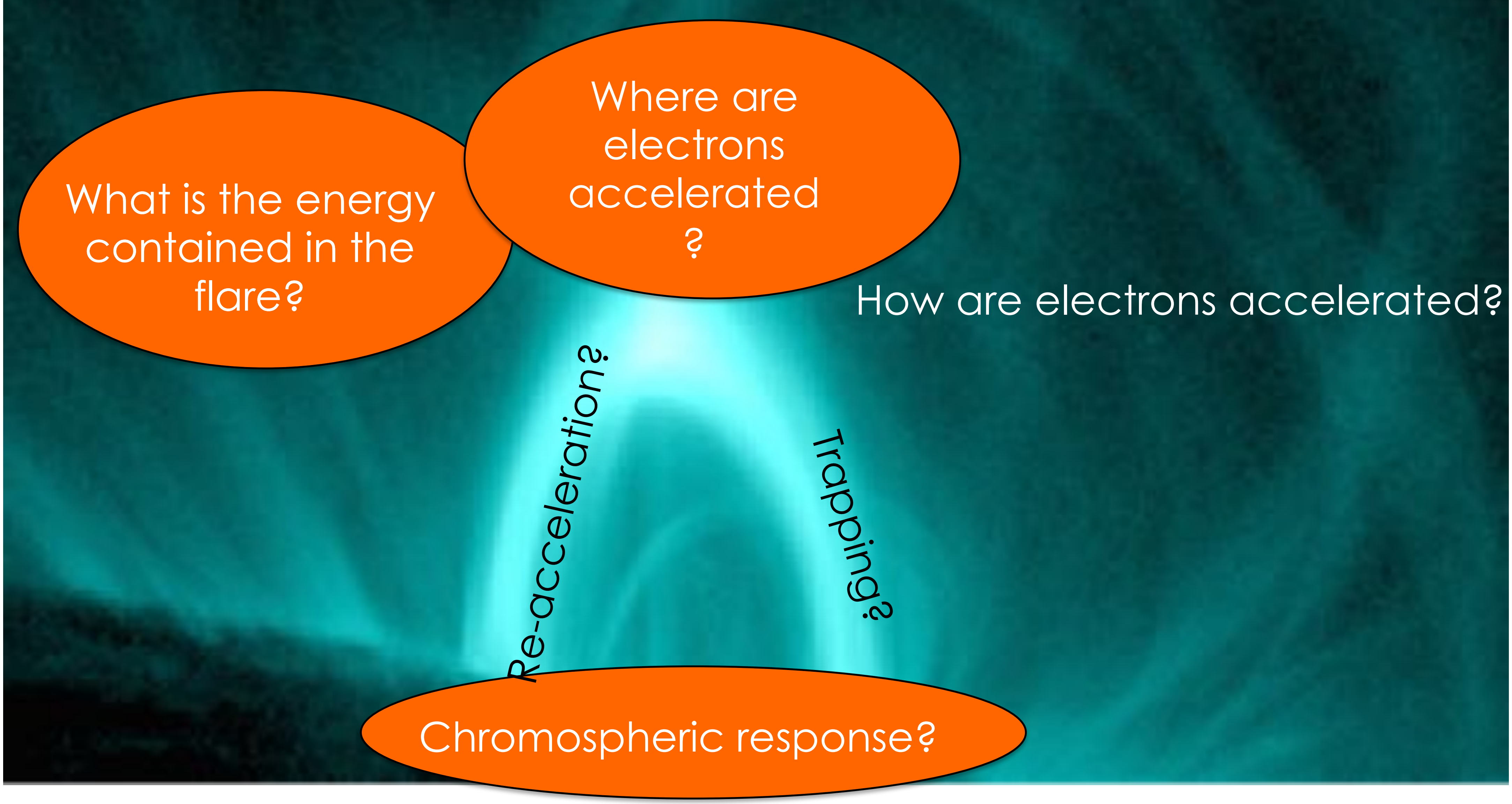

2. …udson Flare Cartoon

…kele…

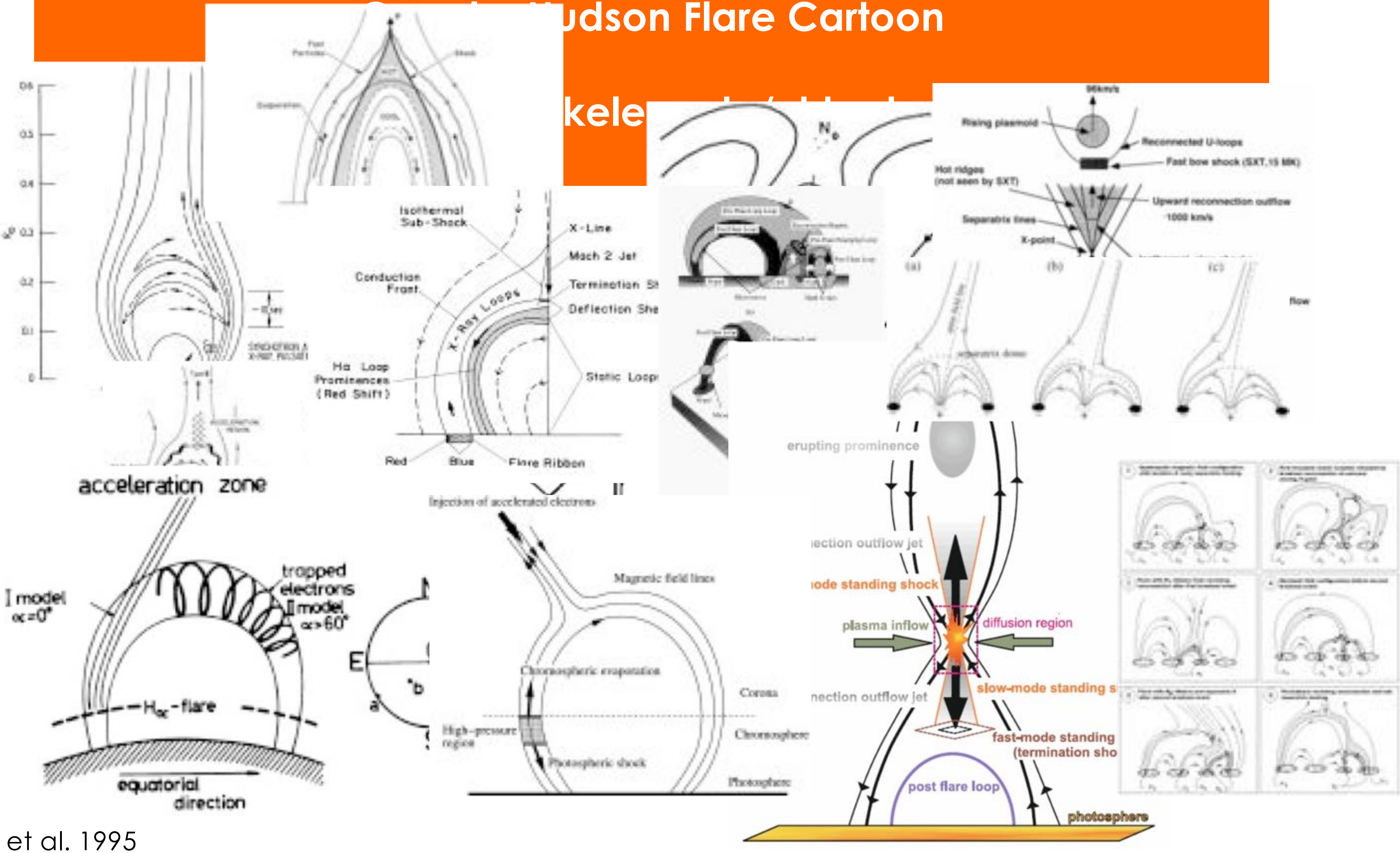

Shibata et al. 1995

X-ray and EUV emission in the standard solar flare scenario

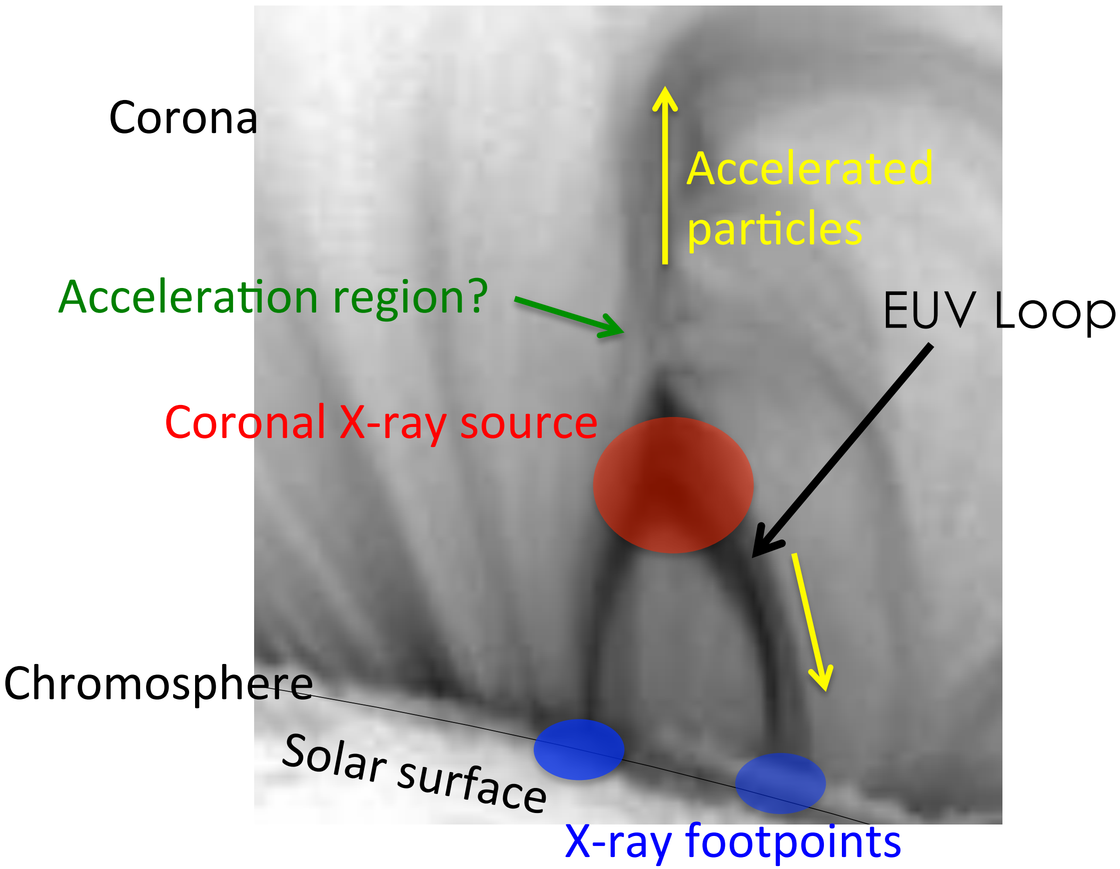

Using observations at X-ray and (E)UV wavelengths we can investigate many aspects of a flare:

- **Hard X-rays**: acceleration region, spectrum of accelerated electrons, and total non-thermal energy
- **SXR/EUV**: chromospheric, transition region, and coronal response, plasma heating
- **optical/UV**: photospheric, chromospheric, and transition region response, plasma flows

3. Emission mechanisms at X-ray and EUV wavelengths

Emission mechanism: bremsstrahlung

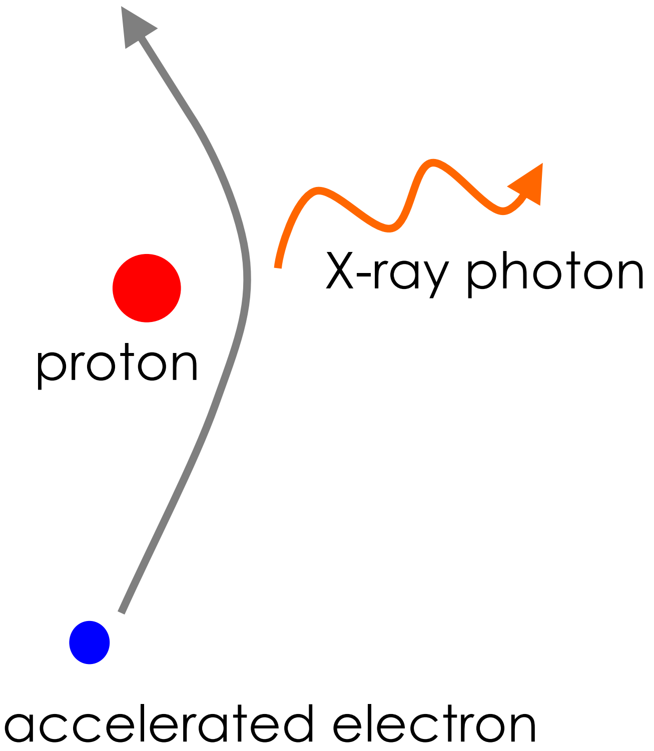

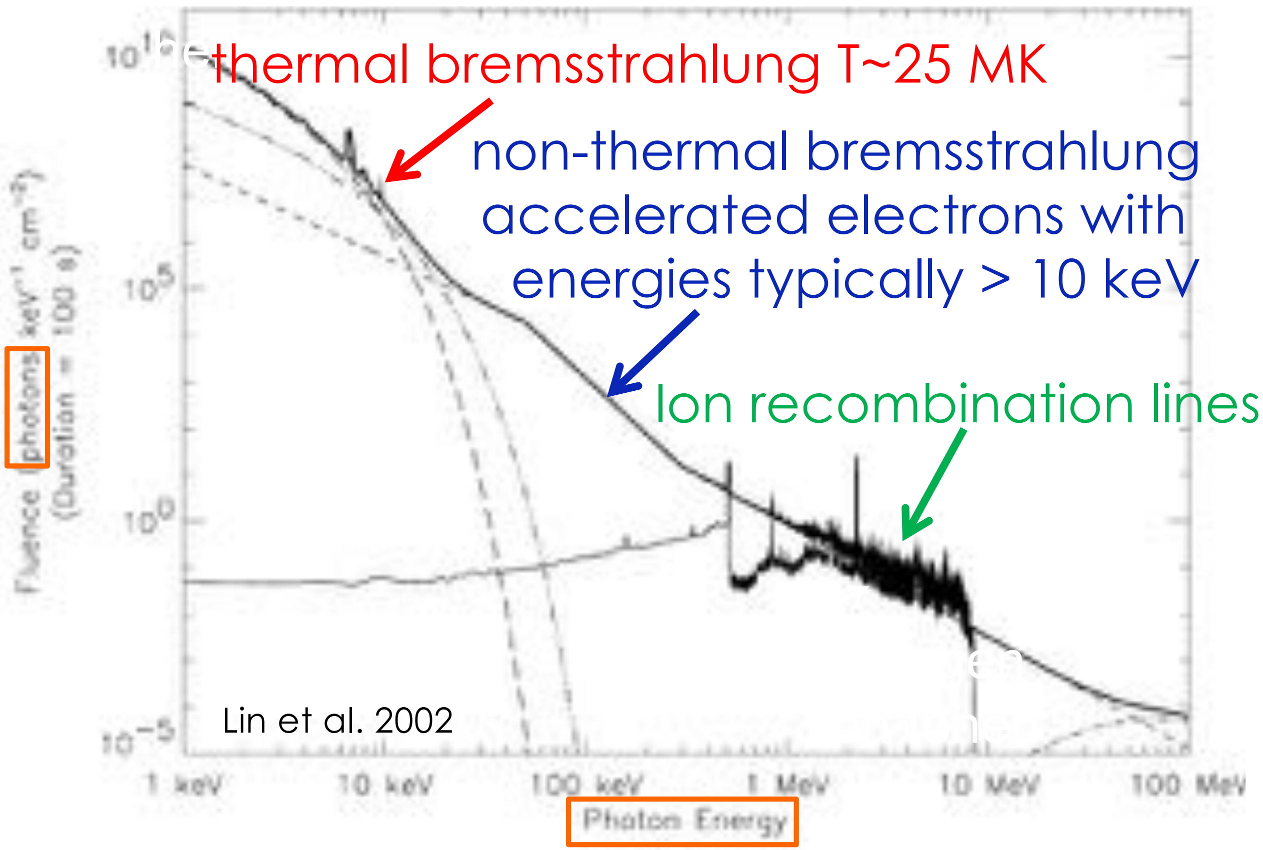

Idealized X-ray flare spectrum

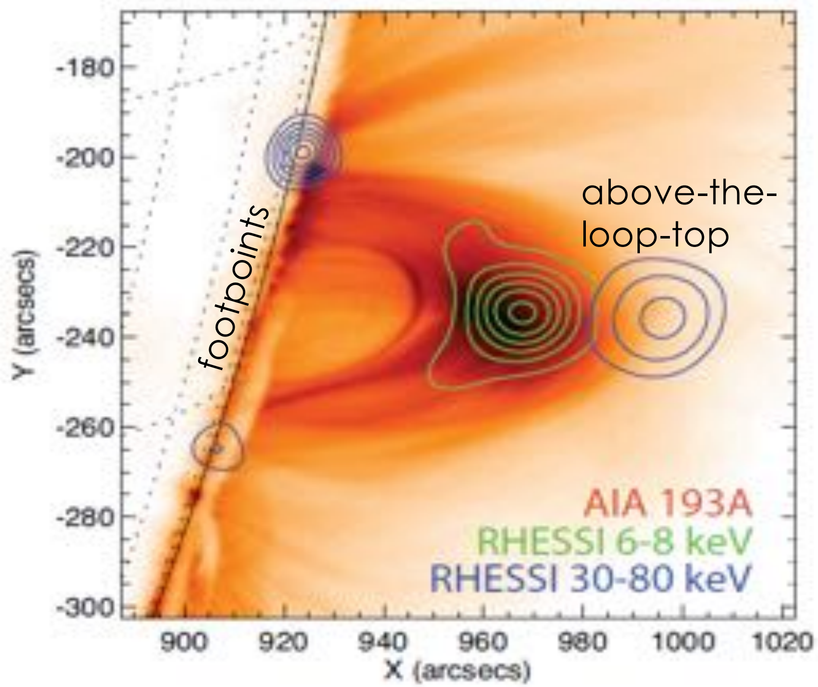

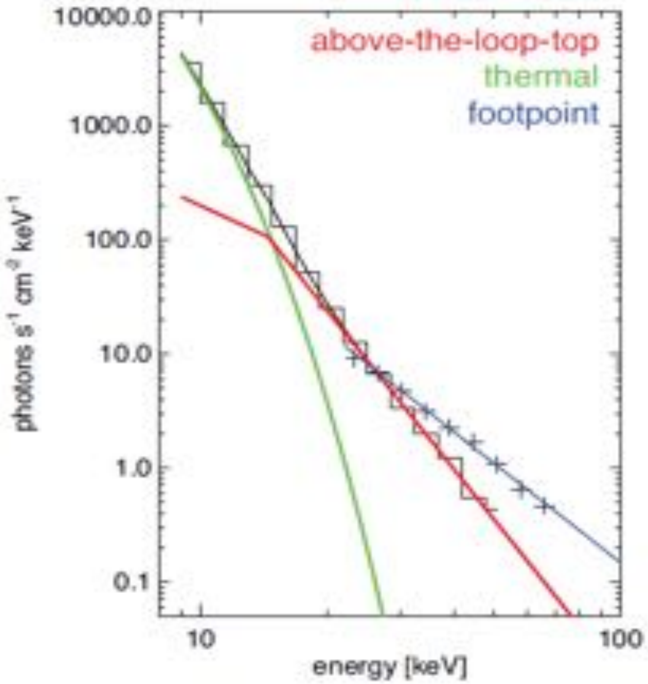

Reuven Ramaty High Energy Solar Spectroscopic Imager (RHESSI)

Krucker & Battaglia 2014

Non-thermal bremsstrahlung from flare accelerated electrons
number of electrons, total non-thermal energy, acceleration region

Thermal bremsstrahlung: temperature and emission measure of heated plasma

EUV line emission

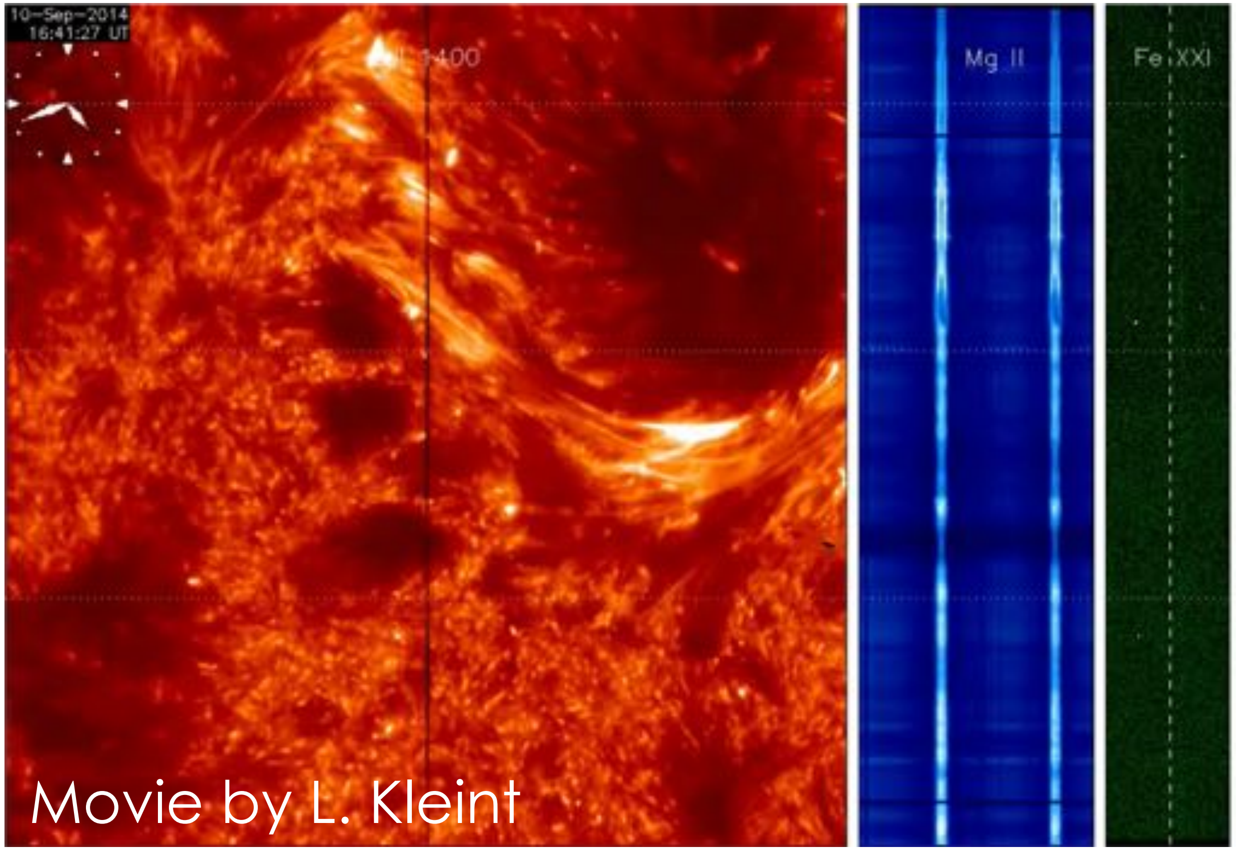

Interface Region Imaging Spectrograph (IRIS)

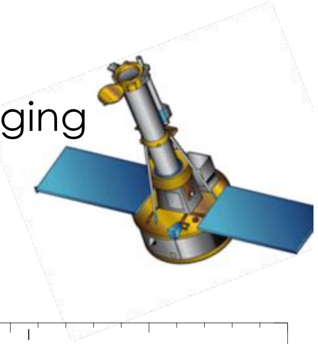

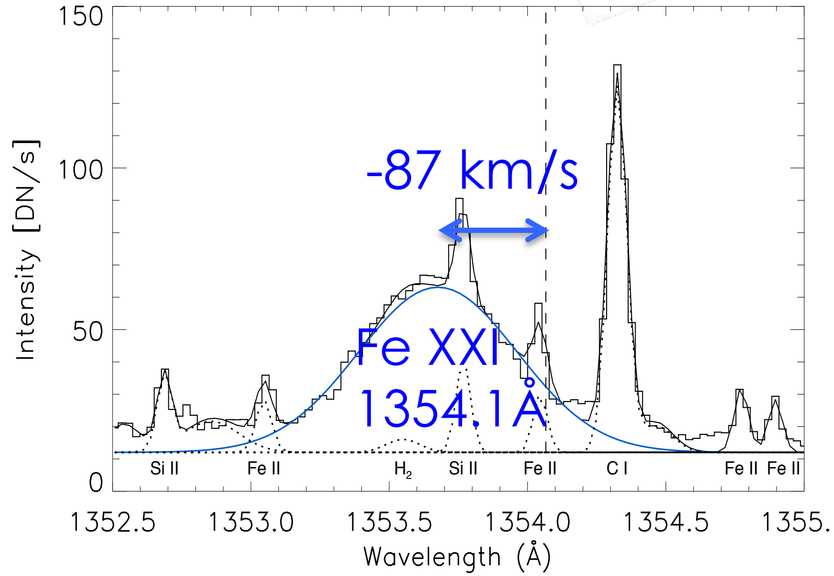

Emission from partially ionized ions in the solar atmosphere.
Different lines are formed under different conditions (temperature, density).
Doppler shifts indicate upflowing and downflowing plasma
Diagnostic of atmospheric response (from photosphere to corona) to flare energy input

4. Electron acceleration: Distribution and energies of accelerated electrons from simultaneous EUV and X-ray analysis

RHESSI photon spectrum

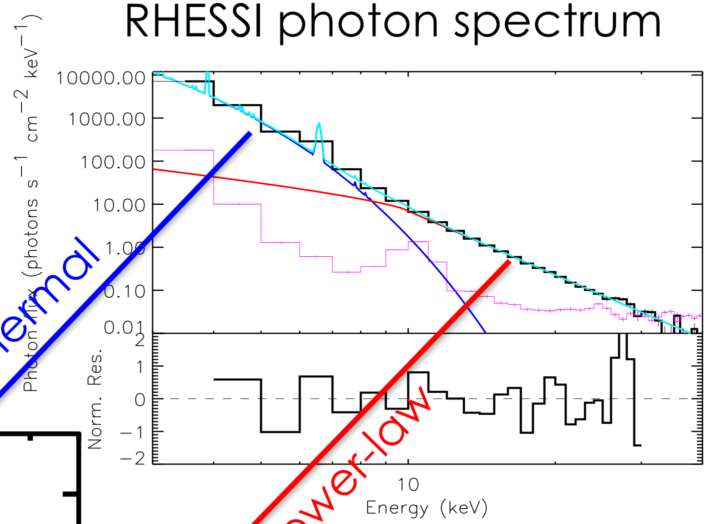

The challenge: infer mean electron flux spectrum <nVF> over largest possible energy range

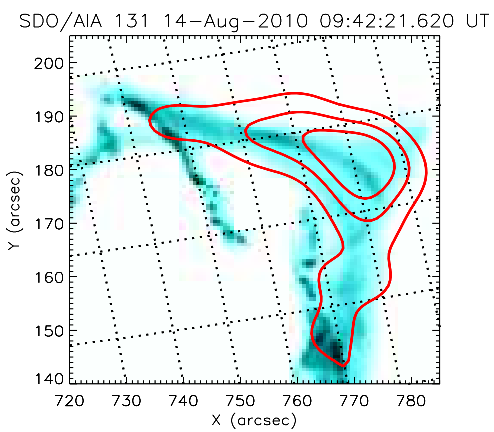

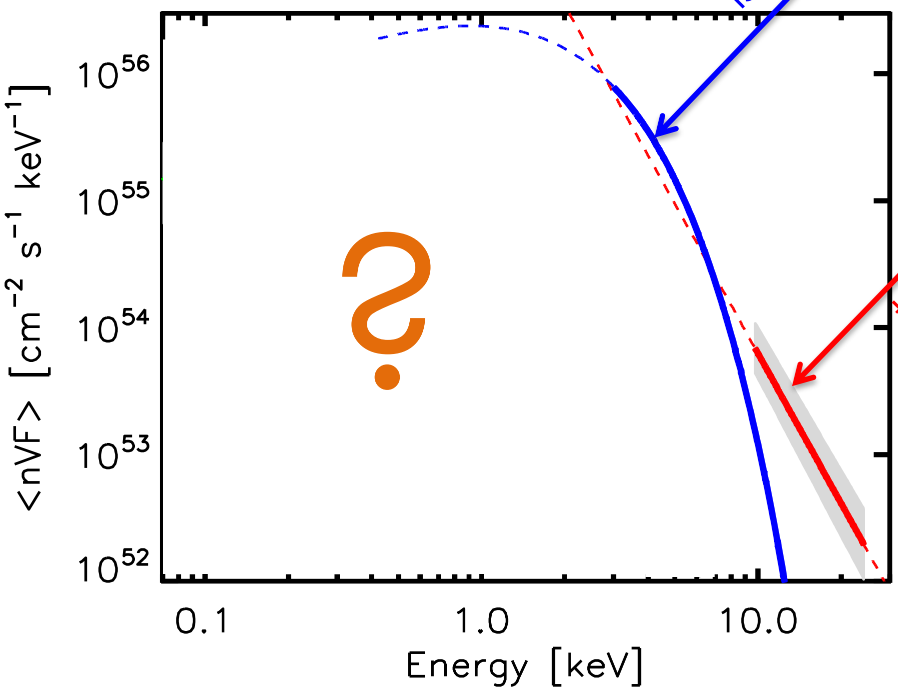

Mean electron flux spectrum from RHESSI observations

→ Can use AIA differential emission measure!

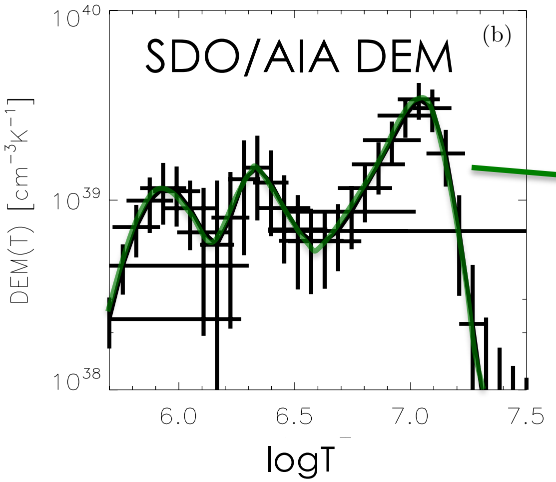

DEM from regularized inversion
(Hannah & Kontar 2012)

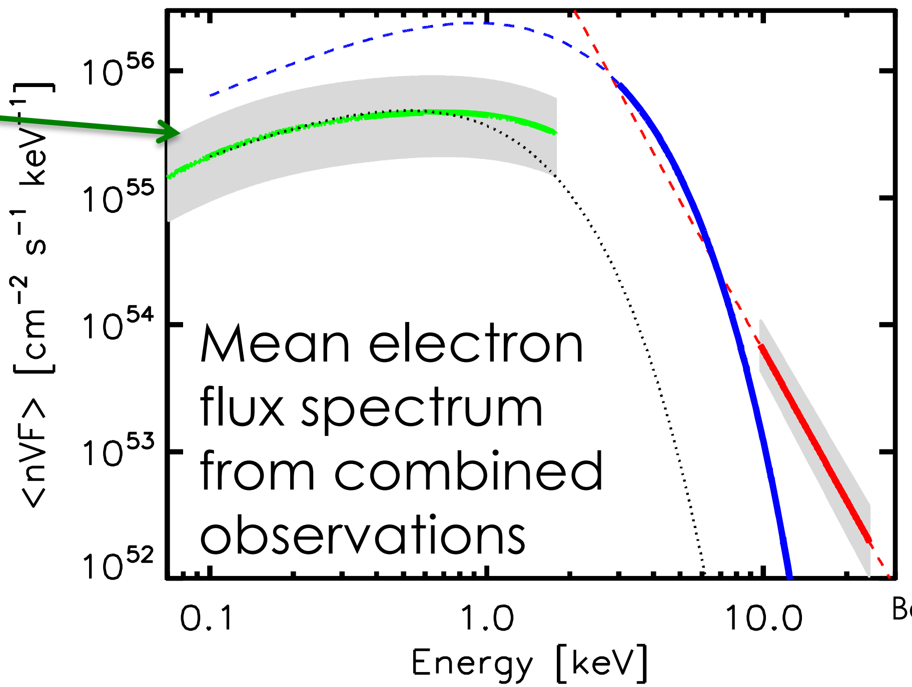

Battaglia & Kontar 2013

<nVF> is directly related to DEM: $\boxed{\langle nVF \rangle} = \frac{2^{3/2} E}{(\pi m_e)^{1/2}} \int_0^\infty \frac{\boxed{\xi(T)}}{(k_B T)^{3/2}} \exp(-E/k_B T)\, dT.$

→ Combining AIA with RHESSI we can extend the energy range down to ~ 0.1 keV

→ Can use AIA differential emission measure!

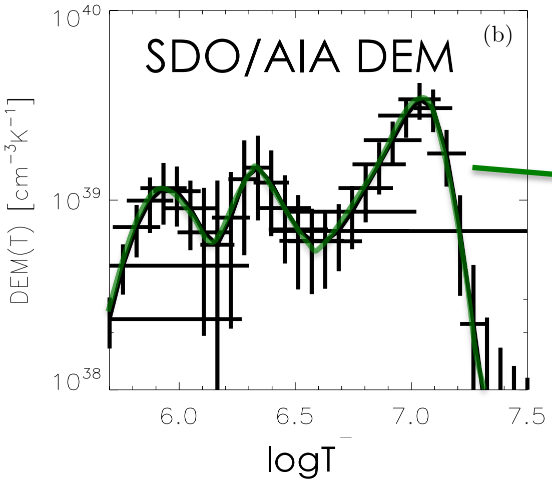

DEM from regularized inversion
(Hannah & Kontar 2012)

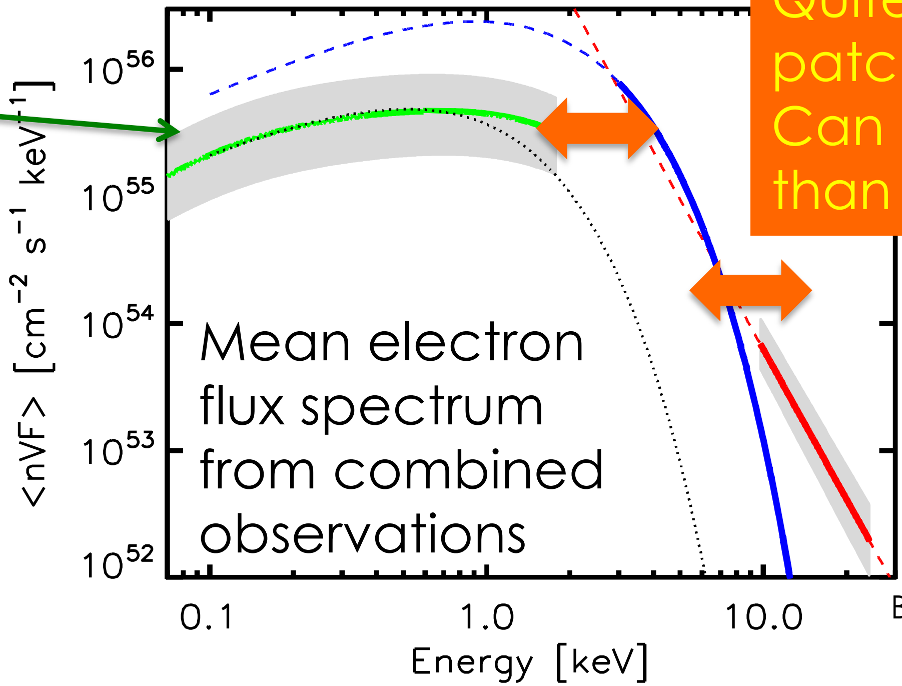

Quite the patchwork. Can do better than that!

Battaglia & Kontar 2013

<nVF> is directly related to DEM: $\boxed{\langle nVF\rangle} = \frac{2^{3/2}E}{(\pi m_e)^{1/2}} \int_0^\infty \frac{\boxed{\xi(T)}}{(k_B T)^{3/2}} \exp(-E/k_B T)\, dT.$

→ Combining AIA with RHESSI we can extend the accessible energy range down to ~ 0.1 keV

Simultaneous fitting of RHESSI and AIA data (Motorina & Kontar 2015)

Ingredients:

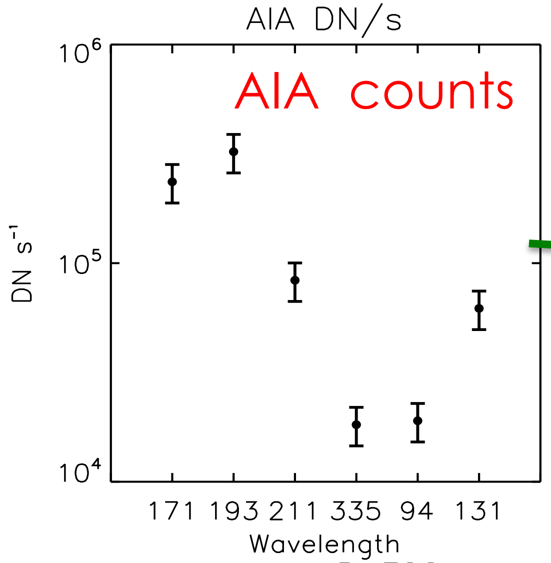

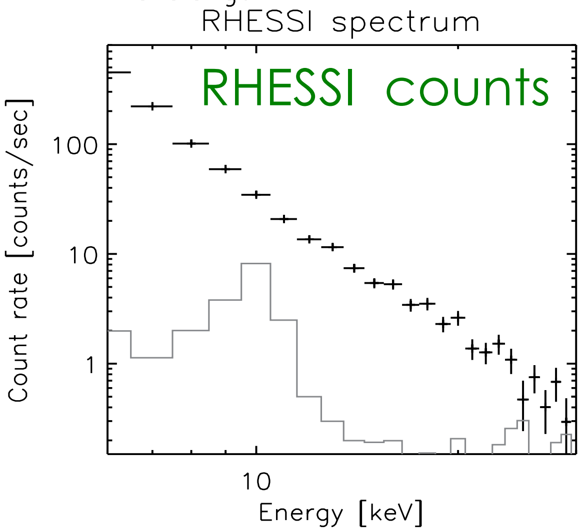

Fitfunction
$\mathcal{I}$(RHESSI, AIA)~$\mathcal{F}$(electron distribution)

$$\begin{pmatrix} R & E & S & P \\ O & N & S & E \\ M & A & T & R \\ I & X & & \end{pmatrix}$$

Combined temperature response matrix

Simultaneous fitting of RHESSI and AIA data (Motorina & Kontar 2015)

Ingredients:

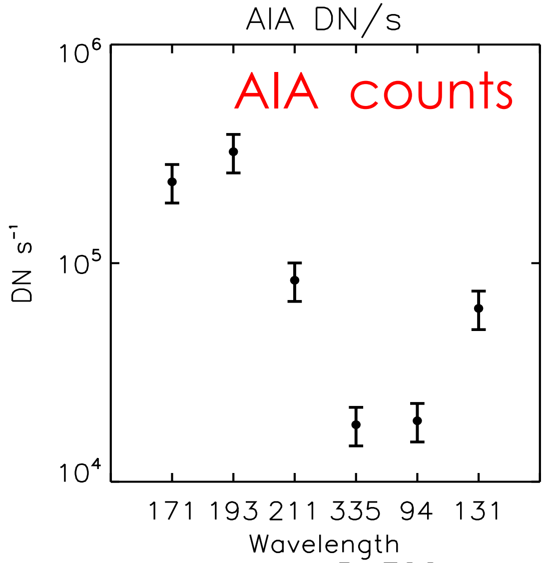

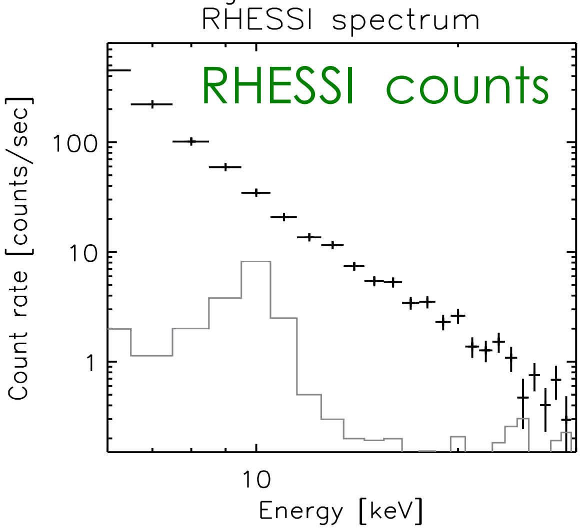

Fitfunction
$\mathcal{I}$(RHESSI, AIA)~$\mathcal{F}$(electron distribution)

$$\begin{pmatrix} R & E & S & P \\ O & N & S & E \\ M & A & T & R \\ I & X & & \end{pmatrix}$$

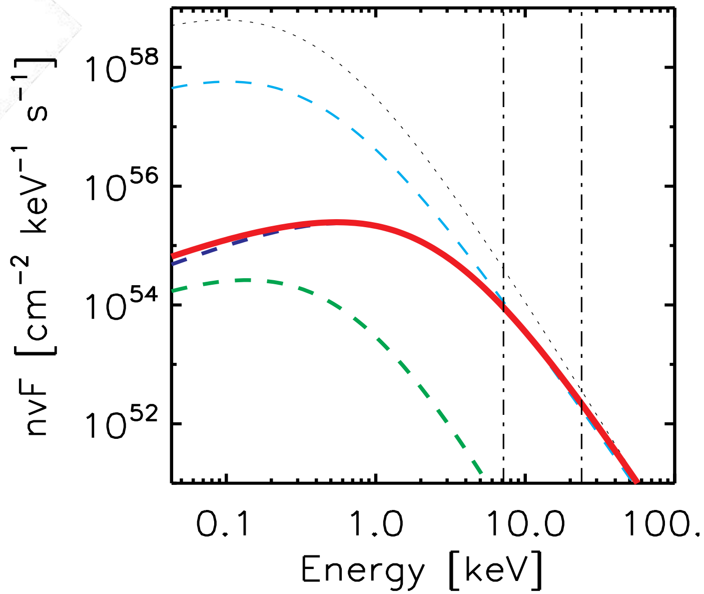

Combined temperature response matrix

- Treat RHESSI and AIA data as one dataset

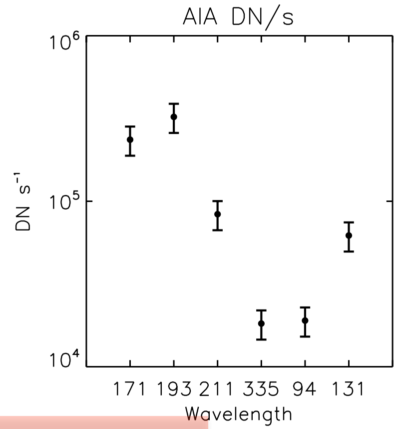

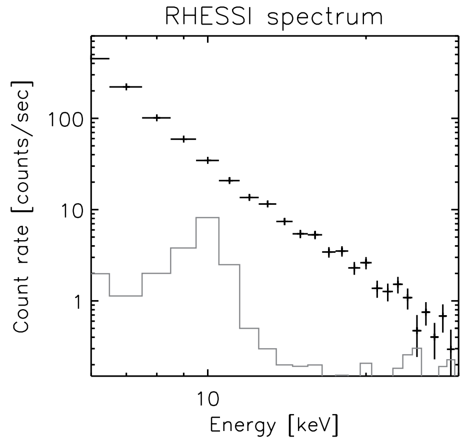

Detected X-ray or EUV signal is

$$g_i = R_{ij}\xi_j dT_j$$

signal = temperature response x DEM x temperature bin width

- Generate one temperature response matrix

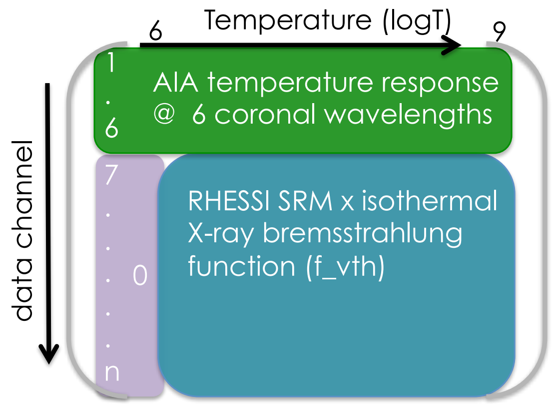

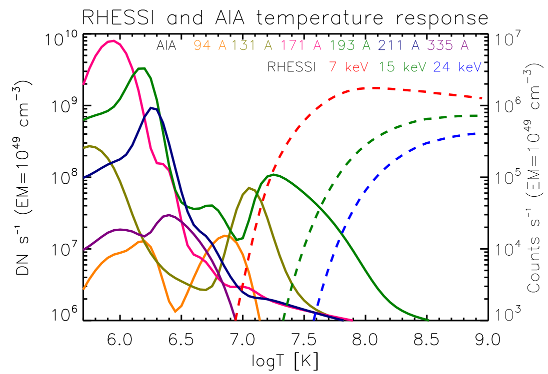

- Forward-fit model DEM

- Find electron flux distribution from DEM

$$\langle nVF\rangle = \frac{2^{3/2}E}{(\pi m_e)^{1/2}}\int_0^\infty \frac{\xi(T)}{(k_BT)^{3/2}}\exp(-E/k_BT)\,dT.$$

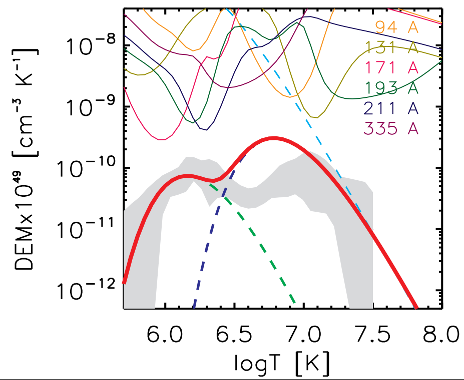

Fitfunction: kappa-distribution

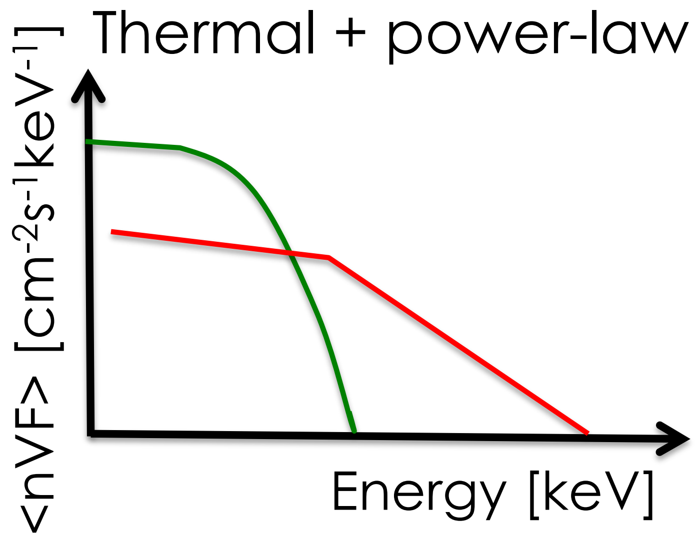

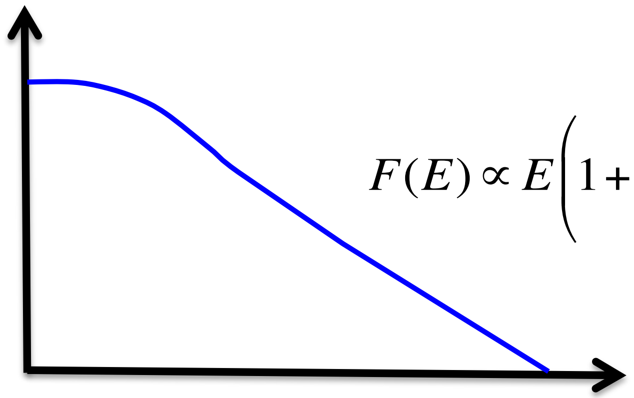

$$F(E) \propto E\left(1+\frac{E}{k_B T_\kappa}(\kappa-1.5)\right)^{-(\kappa+1)}$$

→ T, EM, γ, flux normalization, E_{cut}

→ T_κ, EM_κ, κ

Why kappa?

- Single analytic function to describe whole spectrum
- No cutoff needed
- Supported by stochastic acceleration models (e.g. Bian et al 2014)
- Found in multiple RHESSI observations (e.g. Kasparova & Karlicky 2009, Oka et. al. 2013/2015)

AND: Can express kappa-distribution as differential emission measure!

DEM: $$\xi(T) \propto T^{-(\kappa+0.5)} \exp\left(-\frac{T_\kappa}{T}(\kappa-1.5)\right)$$

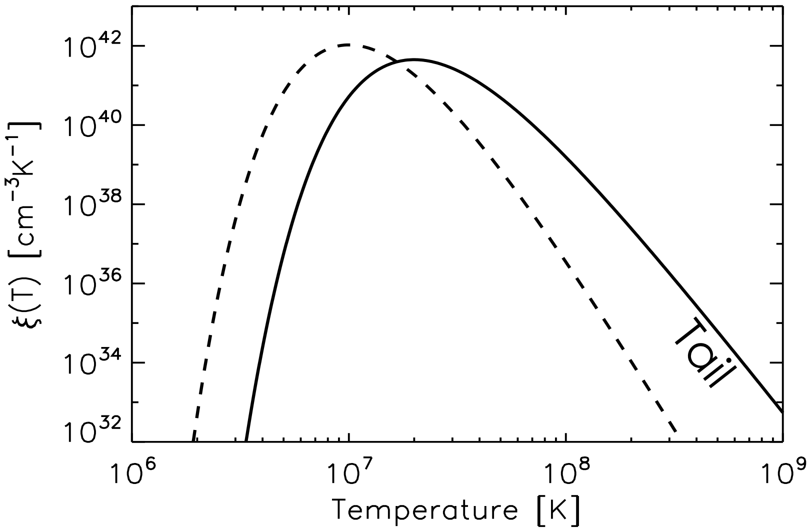

via:

$$\boxed{\langle nVF(E)\rangle} = \frac{2^{3/2}E}{(\pi m_e)^{1/2}} \int_0^\infty \frac{\boxed{\xi(T)}}{(k_B T)^{3/2}} \exp\left(-E/k_B T\right) \mathrm{d}T$$

gives:

$$\langle nVF(E)\rangle = n^2 V \frac{2^{3/2}}{(\pi m_e)^{1/2}(k_B T_\kappa)^{1/2}} \frac{\Gamma(\kappa+1)}{(\kappa-1.5)^{1.5}\Gamma(\kappa-1/2)} \frac{E/k_B T_\kappa}{(1+E/k_B T_\kappa(\kappa-1.5))^{\kappa+1}}$$

= kappa-distribution!

Application on single loop flare

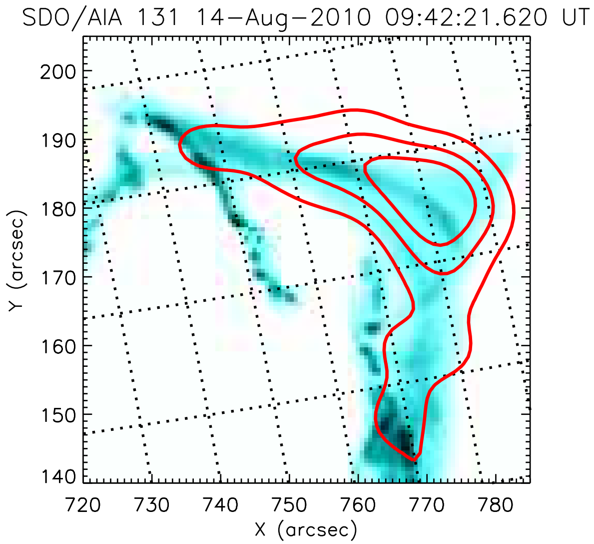

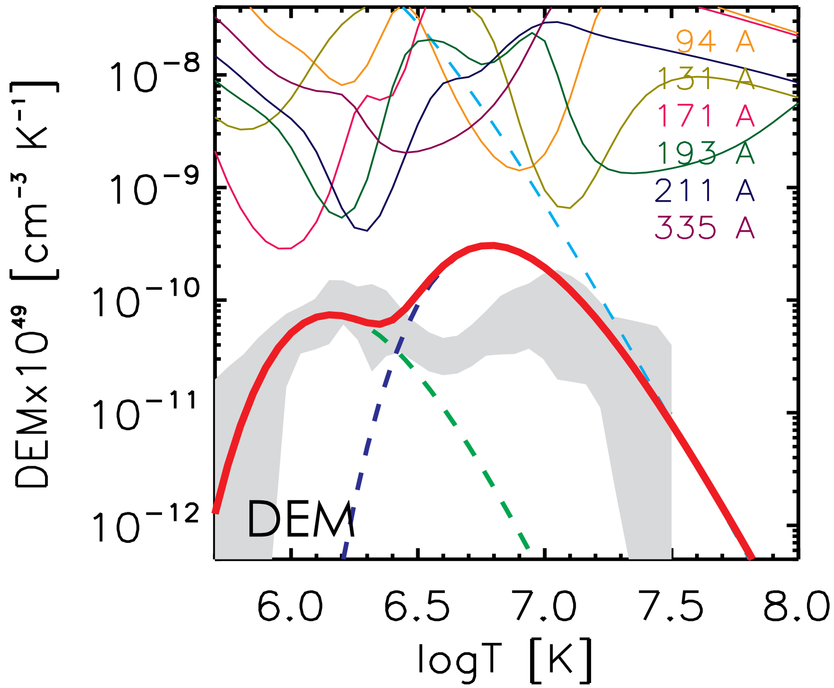

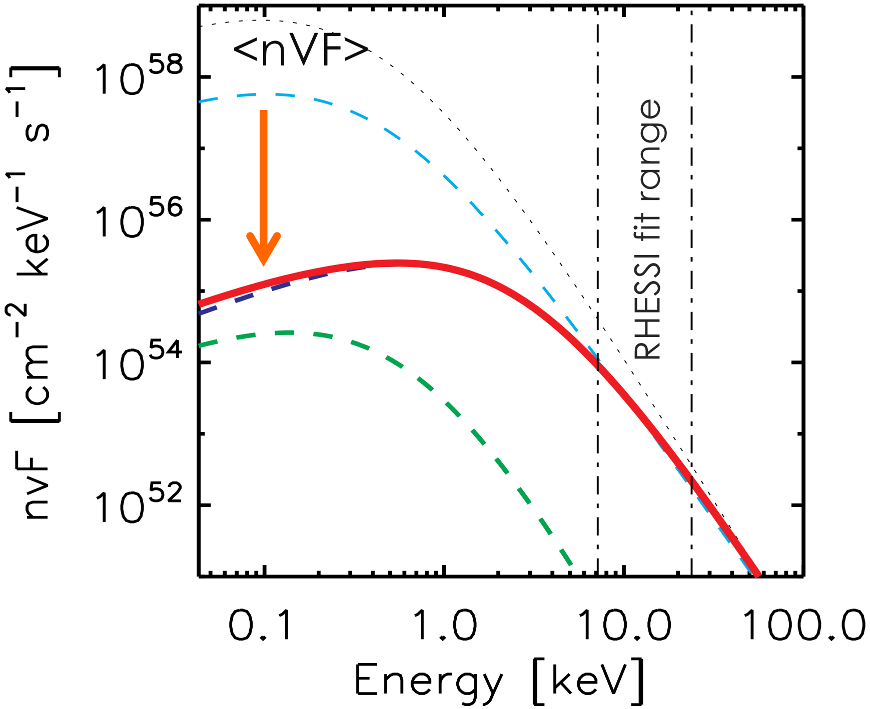

Comparison of mean electron flux spectrum from different fit methods

ξκ(T) on RHESSI data, only
ξκ(T)on RHESSI and AIA data combined
(low and high T component)
AIA DEM from regularized inversion
...... RHESSI thin kappa

Comparison of total energy

Total energy density $U_\kappa = \frac{3}{2} k_B n T_\kappa$

Total energy: $U_\kappa V$ where $V \approx 1.5\text{x}10^{27}$ cm^3

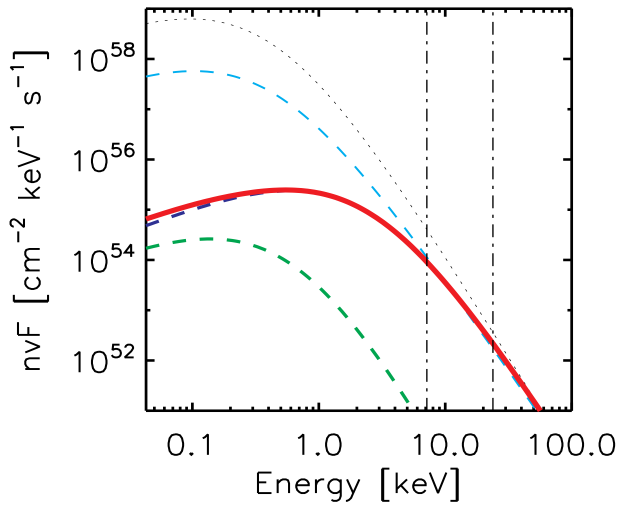

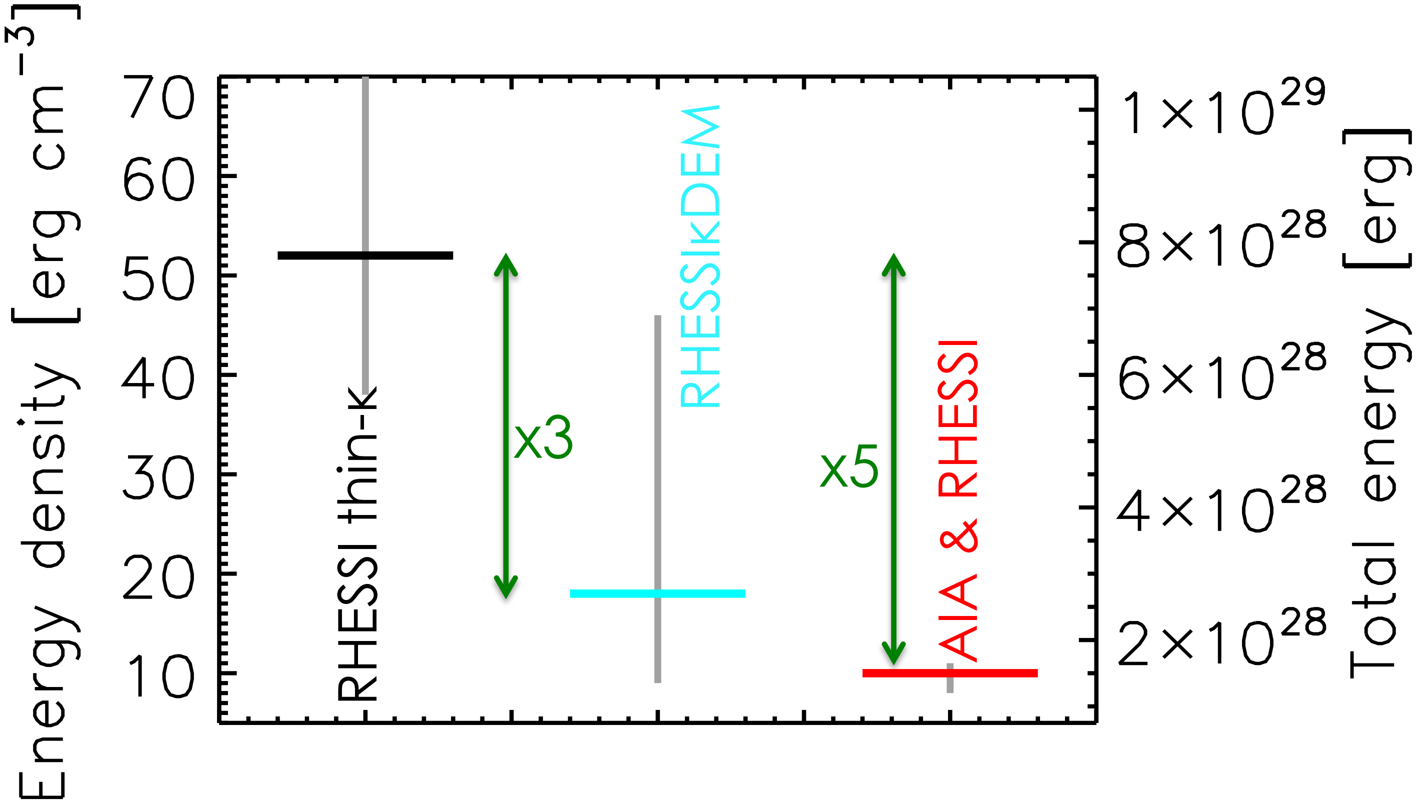

Without low-energy constraint, total energies derived from RHESSI data could be over-estimated by factor ~5

Electron energization in the pre-impulsive phase of SOL2012-07-19T05:58

(see also Liu et al. 2013, Sun et al. 2014, Oka et al. 2015, Huang et al. 2016, Krucker & Battaglia 2014)

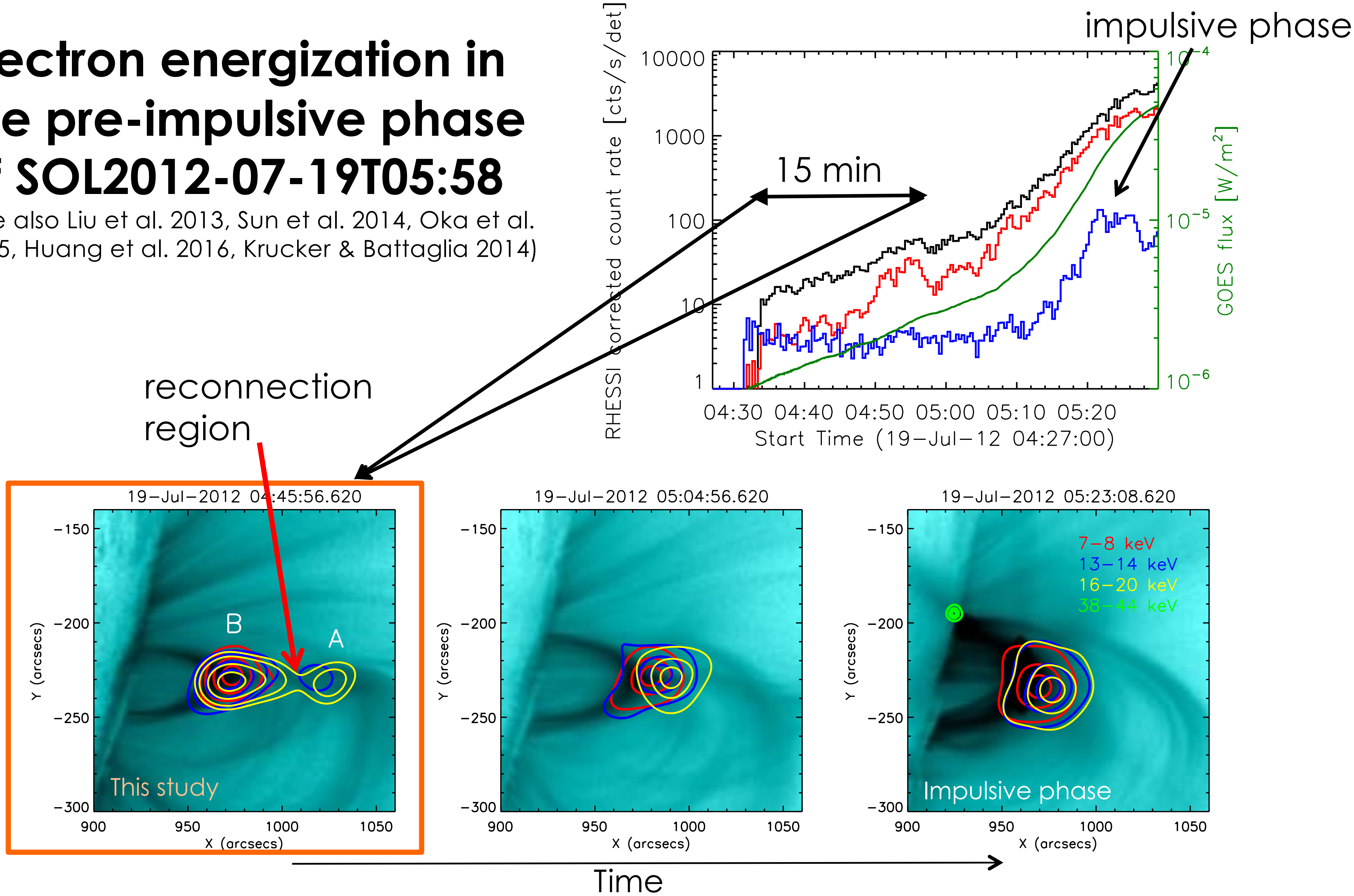

Two sources during the pre-impulsive phase:
One **B**elow the reconnection region, one **A**bove

Use simultaneous EUV and X-ray fitting to investigate time evolution of electron spectrum from to 0.1 keV to 30 keV

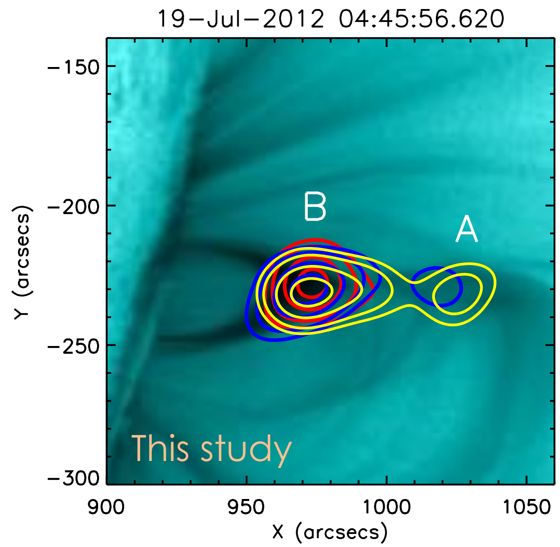

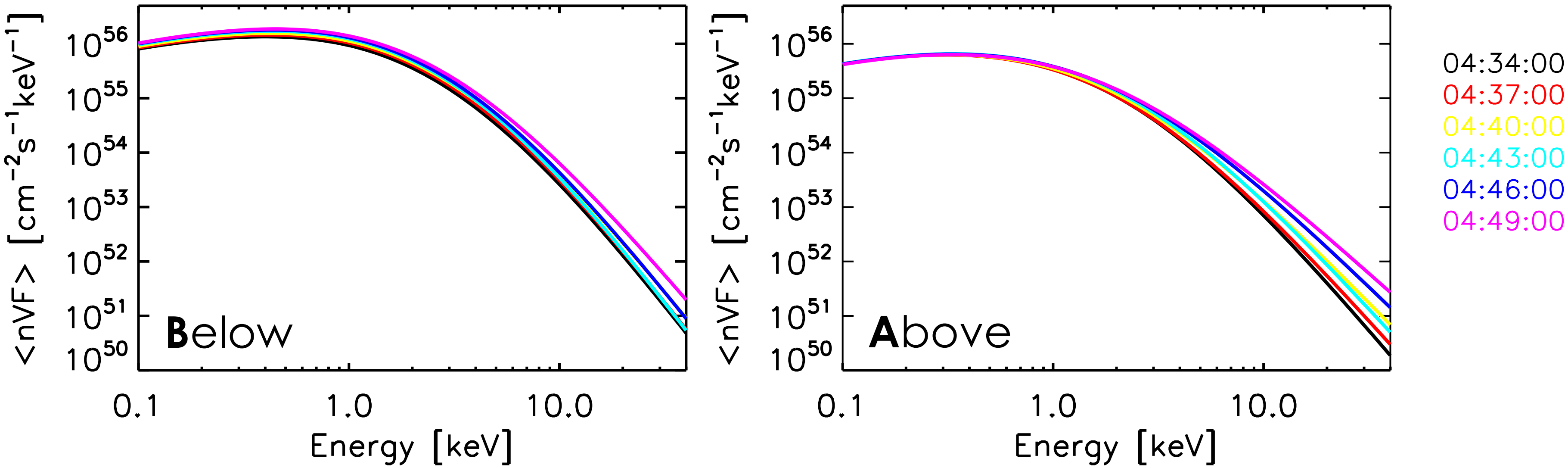

Continuous hardening in Source A vs overall rise in spectrum in Source B

Energies

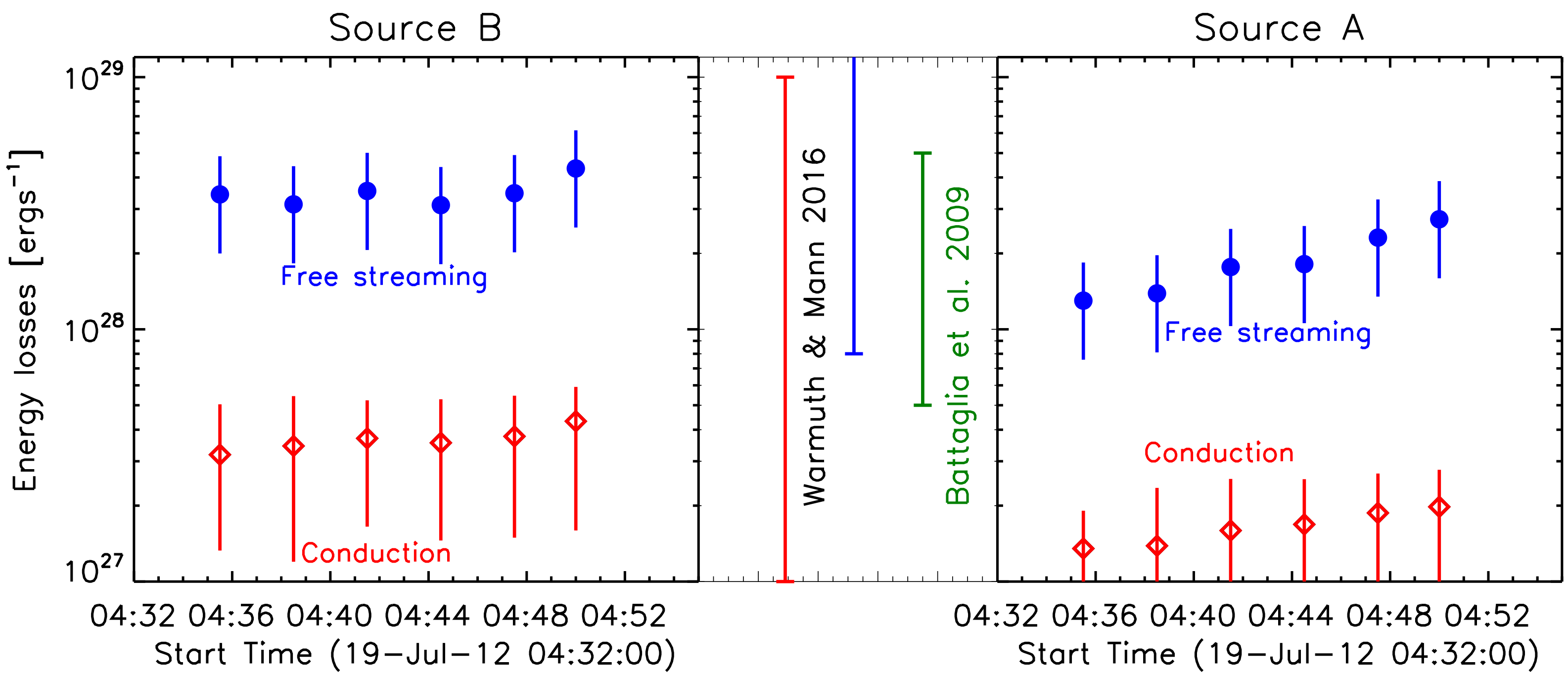

Electron acceleration in source A vs density increase due to evaporation in source B

Energy loss by free streaming electrons dominates in both sources

→ efficient acceleration even in this early flare phase

→ importance of pre-impulsive phase in overall flare energetics

5. Chromospheric response: chromospheric evaporation seen in X-rays and EUV

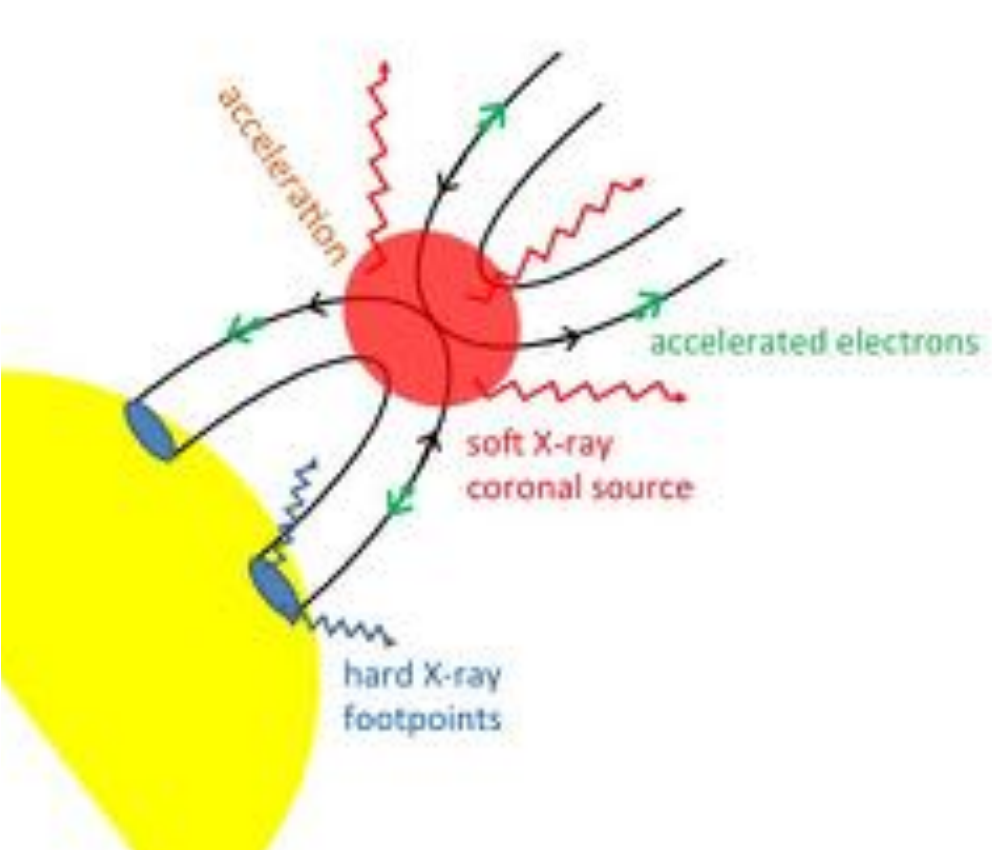

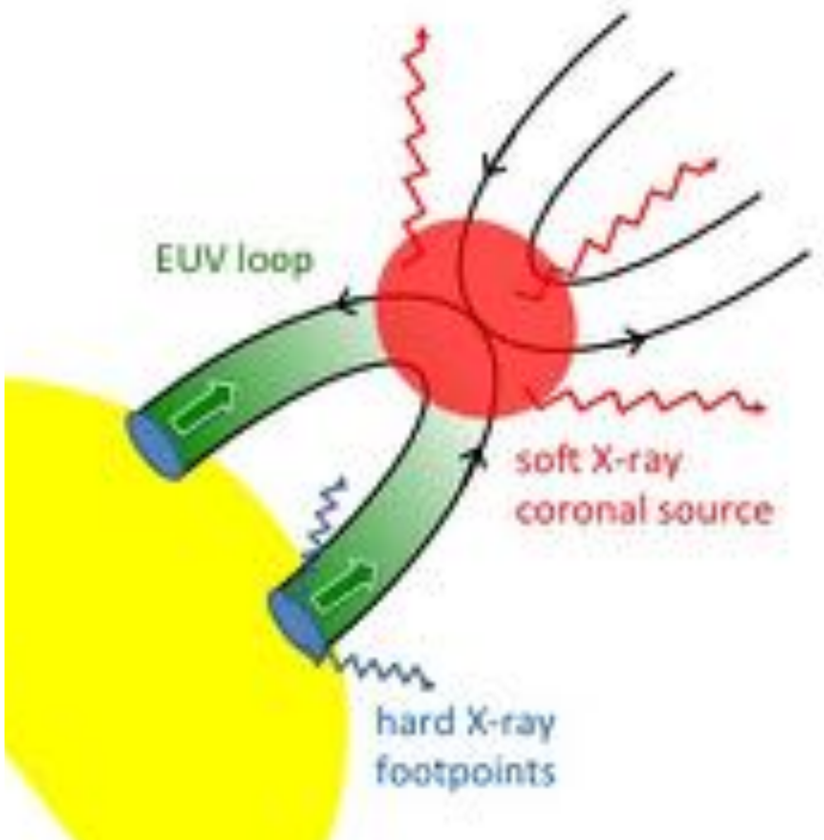

Energy deposition in the chromosphere leads to overpressure and heating causing plasma to expand upward = “chromospheric evaporation”
→ EUV / soft X-ray loops

Milligan et al. 2009: Velocities of evaporating plasma observed with Hinode/EIS

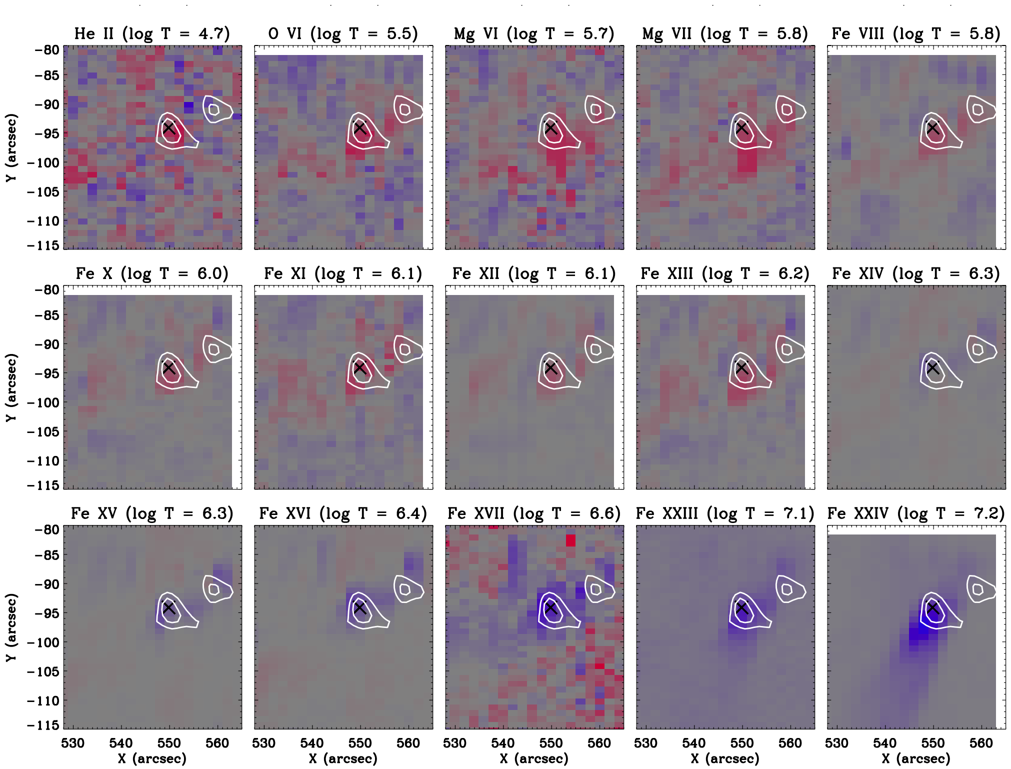

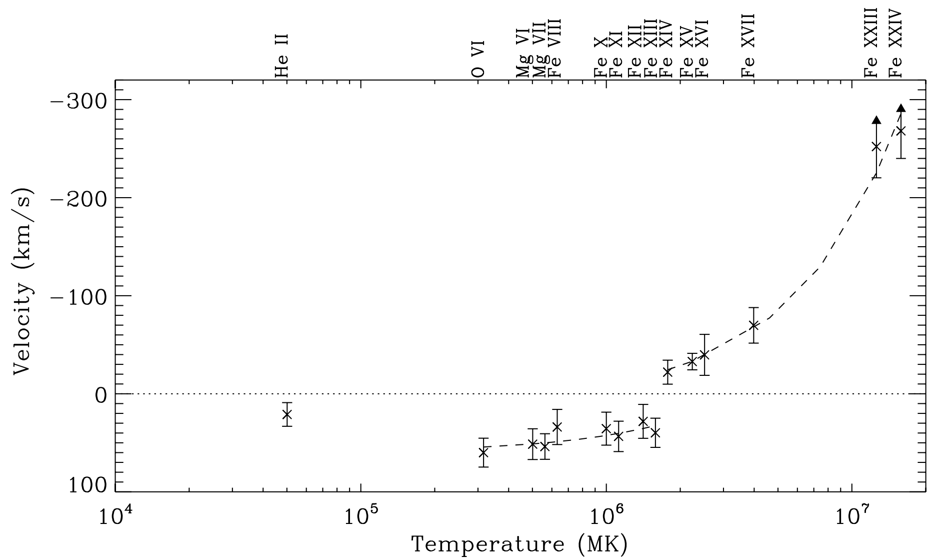

Temporal and spatial correlation of HXR emission with upflows and downflows
→ explosive evaporation driven by non-thermal electron beam

Battaglia et al. 2015: spatial and temporal evolution of chromospheric evaporation with IRIS and RHESSI

GOES X1 flare from 29 March 2014

Two moving flare ribbons
HXR emission during 2 min coinciding with location of ribbons

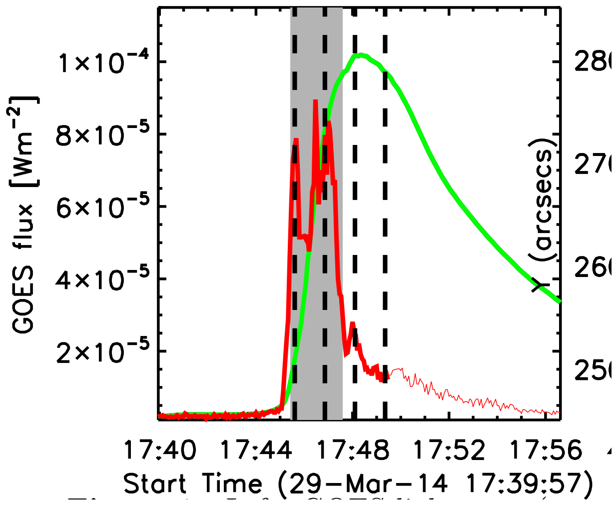

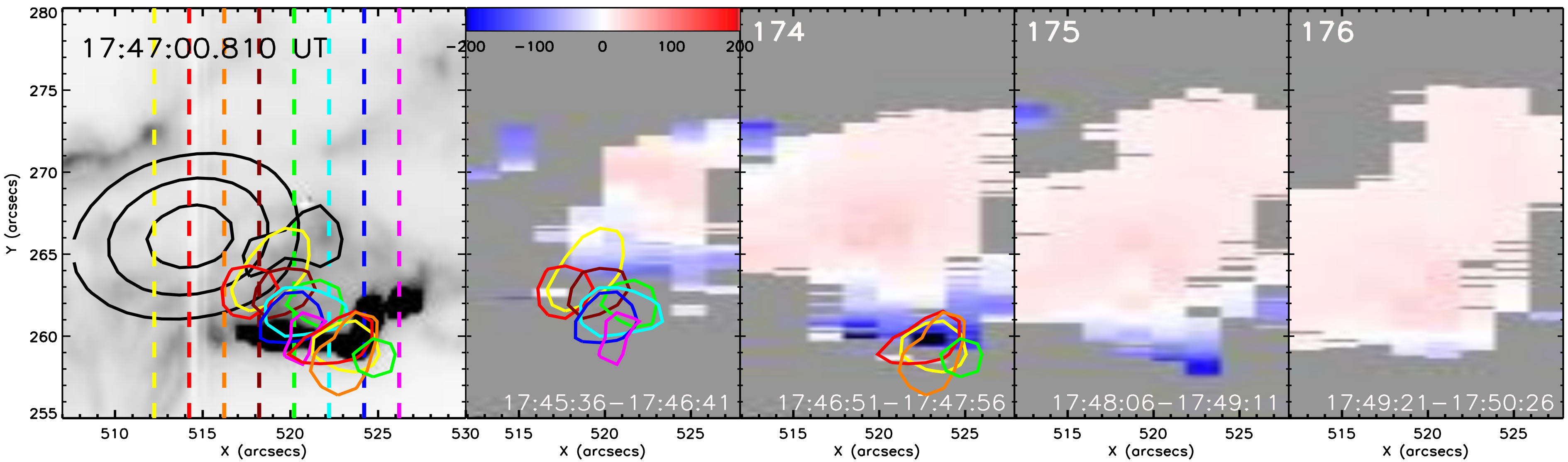

Slit position relative to location of HXR source

→ Upflows along the flare ribbon
→ Maximum speed ~ 200 km/s
→ Sustained several minutes after HXR

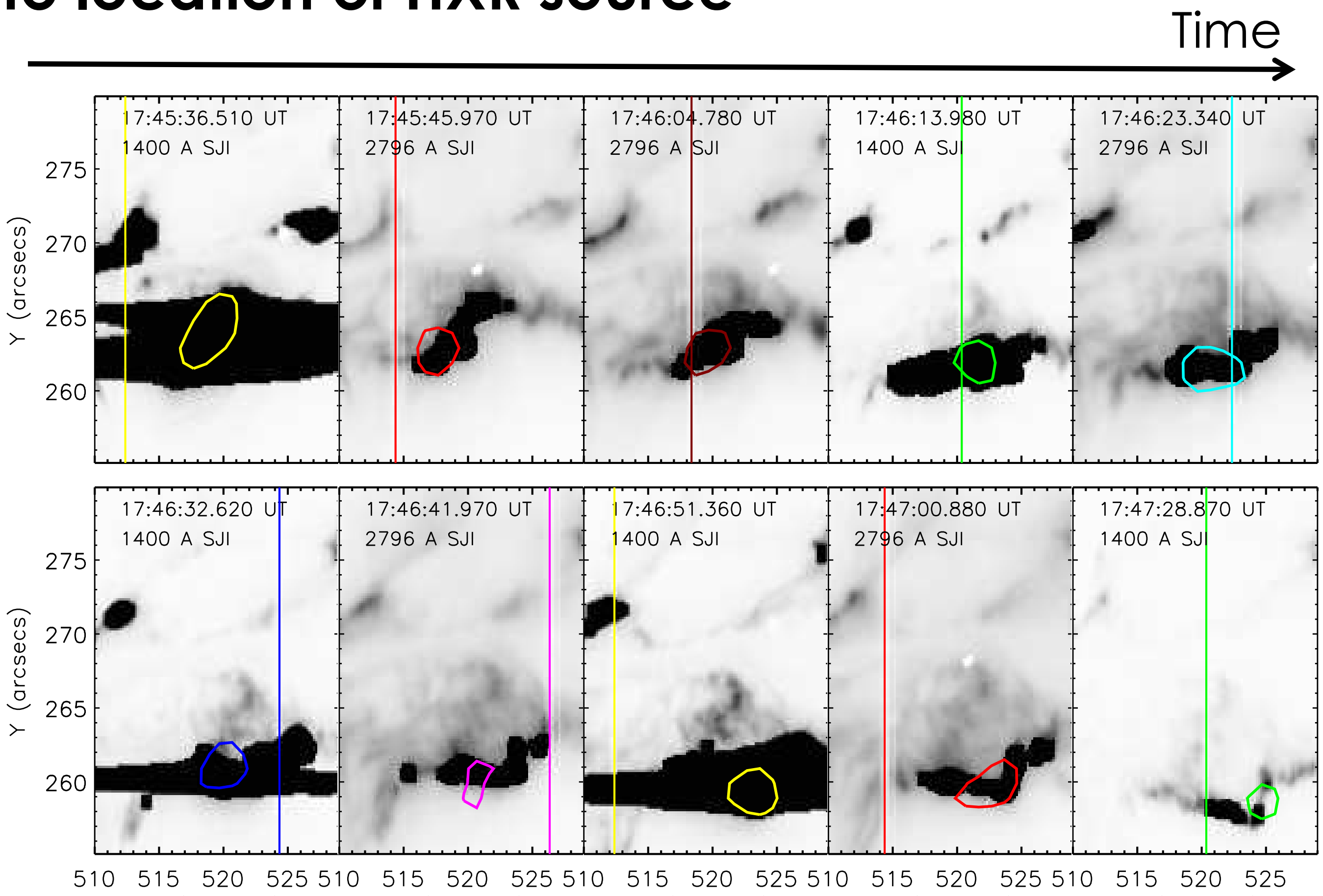

Interpretation
Electron beam driven chromospheric evaporation dominates early in the flare
Evaporation is sustained in later phase due to conductive energy input from hot loop

Summary and conclusion

Signatures of flare accelerated electrons and chromospheric response are readily observed at X-ray and EUV wavelengths

Combining observations at these wavelengths with new data analysis methods is key to understanding particle acceleration and transport in solar flares